

Ultimate precision bound of quantum and sub-wavelength imaging

Cosmo Lupo¹ and Stefano Pirandola^{1,2}

¹York Centre for Quantum Technologies (YCQT), University of York, York YO10 5GH, UK

²Computer Science, University of York, York YO10 5GH, UK

We determine the ultimate potential of quantum imaging for boosting the resolution of a far-field, diffraction-limited, linear imaging device within the paraxial approximation. First we show that the problem of estimating the separation between two point-like sources is equivalent to the estimation of the loss parameters of two lossy bosonic channels, i.e., the transmissivities of two beam splitters. Using this representation, we establish the ultimate precision bound for resolving two point-like sources in an arbitrary quantum state, with a simple formula for the specific case of two thermal sources. We find that the precision bound scales with the number of collected photons according to the standard quantum limit. Then we determine the sources whose separation can be estimated optimally, finding that quantum-correlated sources (entangled or discordant) can be super-resolved at the sub-Rayleigh scale. Our results set the upper bounds on any present or future imaging technology, from astronomical observation to microscopy, which is based on quantum detection as well as source engineering.

PACS numbers: 42.30.-d, 42.50.-p, 06.20.-f

Introduction. Quantum imaging aims at harnessing quantum features of light to obtain optical images of high resolution beyond the boundary of classical optics. Its range of potential applications is very broad, from telescopy to microscopy and medical diagnosis, and has motivated a substantial research activity [1–10]. Typically, quantum imaging is scrutinized to outperform classical imaging in two ways. First, to resolve details below the Rayleigh length (sub-Rayleigh imaging). Second, to improve the way the precision scales with the number of photons, by exploiting non-classical states of light. It is well known that a collective state of N quantum particles has an effective wavelength that is N times smaller than individual particles [11–18]. If N independent photons are measured one expects that the blurring of the image scales as $1/\sqrt{N}$ (known as *standard quantum limit* or *shot-noise limit*), while for N entangled photons one can sometimes achieve a $1/N$ scaling (known as the *Heisenberg limit*).

In this Letter we compute the optimal resolution limit of quantum imaging for estimating the linear or angular separation between two point-like monochromatic sources, by using a linear diffraction-limited imaging device in the far-field regime and within paraxial approximation [19]. In this way, we determine the ultimate capabilities of quantum light for boosting the resolution of optical imaging, setting the upper bound on any present or future imaging technology. We show that the ultimate precision bound scales with the number of photons according to the standard quantum limit, for an arbitrary state of the sources. We then study the precision achievable for sources which are in thermal, discordant or entangled states. We determine the optimal entangled states that saturate the bound and we show that sources of quantum-correlated light yield optimal imaging of sub-Rayleigh features, allowing for higher resolution below the Rayleigh length. Our findings generalize the seminal Ref. [10] which has led to several experimental advances in quantum imaging [20–23].

To achieve our results, we estimate the ultimate precision bound in terms of the quantum Fisher information. The ultimate error of any unbiased estimator of the separation s between two sources is given by the quantum Cramér-Rao

bound [12, 13]

$$\Delta s \geq \frac{1}{\sqrt{\text{QFI}_s}}, \quad (1)$$

where QFI_s is the quantum Fisher information. The latter is a function of s , of the features of the optical imaging system, and of the state of the light emitted by the sources. Here we show that a linear diffraction-limited imaging system in the paraxial approximation is equivalent to a pair of beam splitters, whose transmissivities are functions of the separation (see Fig. 1). Thus, we reduce the estimate of the separation to the estimate of the transmissivity of a beam splitter [24–30]. In this way, not only we are able to compute the quantum Fisher information for any pair of sources but we also determine the optimal sources that saturate the ultimate precision bound.

The quantum model. Consider the canonical annihilation and creation operators, c_1, c_1^\dagger and c_2, c_2^\dagger , describing two monochromatic point-like sources. The sources are separated by distance s and lay on the object plane orthogonal to the optical axis at position $-s/2$ and $s/2$. The imaging system maps the source operators into the image operators a_1, a_1^\dagger and a_2, a_2^\dagger , describing the optical field on the image screen. Without loss of generality, we assume that the optical system has unit magnification factor. This implies that the point spread function has the form $T(x, y) = \sqrt{\eta} \psi(x - y)$, where x and y are respectively the coordinates on the image and object plane, ψ is a function on the image plane with unit L_2 -norm, and η is an attenuation factor. In particular, the image operators read

$$a_1^\dagger = \int dx \psi(x + s/2) a_x^\dagger, \quad (2)$$

$$a_2^\dagger = \int dx \psi(x - s/2) a_x^\dagger, \quad (3)$$

where a_x, a_x^\dagger are the canonical creation and annihilation operators for the field at location x on the image screen.

The image modes are distorted and attenuated versions of the source modes. In fact, the optical imaging system trans-

forms the source operators as [31]

$$c_1 \rightarrow \sqrt{\eta} a_1 + \sqrt{1-\eta} v_1, \quad (4)$$

$$c_2 \rightarrow \sqrt{\eta} a_2 + \sqrt{1-\eta} v_2, \quad (5)$$

where v_1, v_2 are auxiliary environmental modes that we will assume to be in the vacuum state (this is a physically reasonable assumption at optical frequencies). Because of the non-zero overlap between the two point spread functions $\psi(x + s/2)$ and $\psi(x - s/2)$, the image operators a_1 and a_2 are not orthogonal, i.e., they do not satisfy the canonical commutation relations. In order to make them orthogonal we take the sum and difference of the above relations, obtaining

$$c_+ := \frac{c_1 + c_2}{\sqrt{2}} \rightarrow \sqrt{\eta_+} a_+ + \sqrt{1-\eta_+} v_+, \quad (6)$$

$$c_- := \frac{c_1 - c_2}{\sqrt{2}} \rightarrow \sqrt{\eta_-} a_- + \sqrt{1-\eta_-} v_-, \quad (7)$$

where $\eta_{\pm} := (1 \pm \delta)\eta$ are transmissivities depending on the image overlap

$$\delta = \text{Re} \int dx \psi^*(x + s/2) \psi(x - s/2) \quad (8)$$

between the non-orthogonal modes a_1 and a_2 , and

$$a_{\pm} := \frac{a_1 \pm a_2}{\sqrt{2(1 \pm \delta)}} \quad (9)$$

are orthogonal symmetric and antisymmetric canonical operators on the image plane.

The non-local source modes c_{\pm} are hence independently mapped and attenuated into the image modes a_{\pm} , by means of effective attenuation factors $\eta_{\pm} = (1 \pm \delta)\eta$, as also shown in Fig. 1. Inverting Eqs. (6)-(7) we write

$$a_{\pm} = \sqrt{\eta_{\pm}} c_{\pm} - \sqrt{1-\eta_{\pm}} v_{\pm}. \quad (10)$$

Note that the overlap δ between the two point spread functions is a crucial parameter in our model: it quantifies the diffraction introduced by the imaging optical system, as well as the amount of constructive (destructive) interference in the symmetric (antisymmetric) image modes. Also note that this model is well-defined only for $\eta \leq 1/2$: we remark that this is in accordance with the fact that in the paraxial approximation a point source is always (by definition) imaged in the far-field regime, in which light is attenuated by a factor $\eta \ll 1$ (see, e.g., Refs. [32, 33]) [34].

Our equivalent representation of the imaging process leads to a simple description for the dynamical evolution of the image operators a_{\pm} in terms of the separation s between the source. In fact, we may prove the following.

Lemma 1 *Consider a diffraction-limited linear-optical system creating an image of two point-like sources. The symmetric and antisymmetric image operators a_{\pm} satisfy the following dynamical equations in terms of the separation parameter*

$$\frac{da_{\pm}}{ds} = i\omega_{\pm}[H_{\pm}^{\text{eff}}, a_{\pm}], \quad (11)$$

where H_{\pm}^{eff} are suitable beam splitter-like Hamiltonians and ω_{\pm} are suitable angular frequencies.

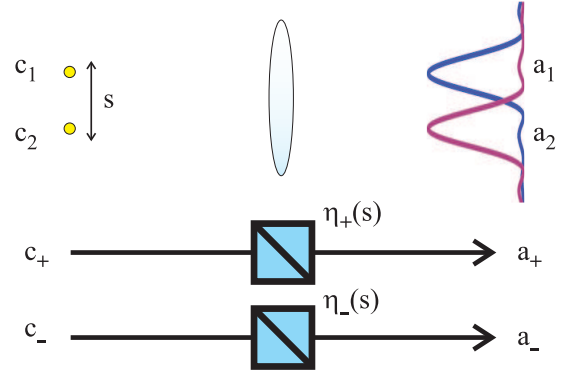


FIG. 1: A diffraction-limited linear-optical system creating an image of two point-like sources (top of the figure) is formally equivalent to a pair of independent beam splitters (bottom of the figure), whose transmissivities are functions of the separation between the sources, with $c_{\pm} = (c_1 \pm c_2)/\sqrt{2}$.

Proof. First of all, from Eq. (10) we may equivalently write $a_{\pm} = e^{i\theta_{\pm} H_{\pm}} c_{\pm} e^{-i\theta_{\pm} H_{\pm}}$, where

$$H_{\pm} = i(c_{\pm}^{\dagger} v_{\pm} - v_{\pm}^{\dagger} c_{\pm}) \quad (12)$$

are two independent beam splitter-like Hamiltonians with rotation angles $\theta_{\pm} = \arccos \sqrt{\eta_{\pm}}$ [35]. In the Heisenberg picture, the dynamics with respect to s is therefore expressed by

$$\frac{da_{\pm}}{ds} = i \frac{d\theta_{\pm}}{ds} [H_{\pm}, a_{\pm}] + \frac{\partial a_{\pm}}{\partial s}. \quad (13)$$

The term with the commutator already describes an effective beam splitter-like transformation. It remains to analyze the term with the partial derivative. After some derivation, we found that the operators $\frac{\partial a_{\pm}}{\partial s}$ are proportional to a pair of corresponding canonical operators b_{\pm} (see Appendix A for details and exact definitions). We obtain

$$\frac{\partial a_{\pm}}{\partial s} = -\frac{\epsilon_{\pm}}{2\sqrt{1 \pm \delta}} b_{\pm}, \quad (14)$$

with

$$\epsilon_{\pm}^2 = \Delta k^2 \mp \beta - \frac{\gamma^2}{1 \pm \delta}, \quad (15)$$

$$\Delta k^2 := \int dx \left| \frac{d\psi(x)}{dx} \right|^2, \quad \gamma := \frac{d\delta}{ds}, \quad (16)$$

$$\beta := \int dx \frac{d\psi(x + s/2)}{dx} \frac{d\psi(x - s/2)}{dx}. \quad (17)$$

From Eqs. (12), (13) and (14) we obtain

$$\frac{da_{\pm}}{ds} = -\frac{d\theta_{\pm}}{ds} v_{\pm} - \frac{\epsilon_{\pm}}{2\sqrt{1 \pm \delta}} b_{\pm}, \quad (18)$$

so that the dynamical equations can be locally written as in Eq. (11), where the angular frequencies are given by

$$\omega_{\pm} = \sqrt{\left(\frac{d\theta_{\pm}}{ds} \right)^2 + \frac{\epsilon_{\pm}^2}{4(1 \pm \delta)}}, \quad (19)$$

and $H_{\pm}^{\text{eff}} = i \left(c_{\pm}^{\dagger} d_{\pm} - d_{\pm}^{\dagger} c_{\pm} \right)$ are beam splitter-like Hamiltonians mixing the source modes c_{\pm} with the auxiliary modes

$$d_{\pm} = \frac{1}{\omega_{\pm}} \left[\frac{d\theta_{\pm}}{ds} v_{\pm} + \frac{\epsilon_{\pm}}{2\sqrt{1 \pm \delta}} b_{\pm} \right]. \quad (20)$$

Note that the parameters ϵ_{\pm}^2 in Eq. (15) contain three terms: (i) γ^2 accounts for the variations of the overlap δ due to changes of the separation s ; (ii) Δk^2 equals the variance of the momentum operator $-i\frac{d}{dx}$ and hence describes translations on the image screen; and (iii) β accounts for interference between the derivatives of the point spread functions.

Upper bound on the quantum Fisher information. With Lemma 1 we have shown that estimating the separation between the sources is equivalent to estimating the angle of rotation of a beam splitter-like transformation. We now obtain the fundamental limits of quantum and sub-Rayleigh imaging by exploiting the fact that the quantum Fisher information for the angle of a beam splitter rotation, when the other input port of the beam splitter is in the vacuum state, is no larger than $4\bar{n}$, where \bar{n} is the mean photon number [24, page 4]. In our setting, the fact that the other beam splitter port is in the vacuum state corresponds to the assumption that the only light entering the optical system is that coming from the sources to be imaged, i.e., we are neglecting any source of background radiation, which is a natural assumption at optical frequencies.

Theorem 2 *Consider two point-like sources with unknown separation s , and emitting a total of $2N$ mean photons, which are observed by an optical system with point spread function $T(x, y) = \sqrt{\eta} \psi(x - y)$ and attenuation η . Then, the quantum Fisher information cannot exceed the upper bound*

$$\text{QFI}_s \leq \frac{2\eta N}{x_R^2} \max \{f_+, f_-\}, \quad (21)$$

where x_R is the Rayleigh length and the f -functions are given by $f_{\pm} := x_R^2 \{c_{\pm}^2 + \gamma^2(1 \pm \delta)^{-1}[1 - (1 \pm \delta)\eta]^{-1}\}$.

Proof. To obtain the upper bound, assume that we can measure not only the image modes a_{\pm} , but also the vacuum modes v_{\pm}, b_{\pm} . Let us denote as $|\psi\rangle_{c_+c_-}$ the state of the light emitted by the sources c_{\pm} . The state of the light at the image screen, together with the state of the auxiliary modes v_{\pm} and b_{\pm} is

$$|\psi'\rangle = (e^{-i\theta_+ H_+} e^{-i\theta_- H_-} |\psi\rangle_{c_+c_-} |0\rangle_{v_+v_-}) |0\rangle_{b_+b_-}. \quad (22)$$

According to Lemma 1, the dynamics with respect to s is described by the effective beam splitter Hamiltonian $H^{\text{eff}} = \omega_+ H_+^{\text{eff}} + \omega_- H_-^{\text{eff}}$. The upper bound on the quantum Fisher information is therefore obtained by the formula [12, 13]

$$\text{QFI}_s \leq 4 \langle \psi' | \Delta^2 H^{\text{eff}} | \psi' \rangle. \quad (23)$$

The calculation of the right hand side of this inequality is reported in Appendix B, where we use the upper bound of Ref. [24]. In particular, if source c_{\pm} emits N_{\pm} mean photons, i.e., $\langle \psi | c_{\pm}^{\dagger} c_{\pm} | \psi \rangle = N_{\pm}$, then we obtain

$$\text{QFI}_s \leq \frac{\eta}{x_R^2} (N_+ f_+ + N_- f_-). \quad (24)$$

Now, if we fix the total number of photons $2N = N_+ + N_-$, then the maximum is obtained by either $(N_+, N_-) = (2N, 0)$ or $(N_+, N_-) = (0, 2N)$, yielding the bound of Eq. (21). ■

The upper bound in Eq. (21) is proportional to the mean number of collected photons $2\eta N$, according to the standard quantum limit. This property is directly inherited from the optimal estimation of a lossy bosonic channel. As expected, the upper bound is inversely proportional to the square of the Rayleigh length x_R , in accordance to the fact that a smaller Rayleigh length allows for higher resolution. Also note that the bound depends on the two functions f_+ and f_- which are the contributions of the non-local source modes c_+ and c_- to the quantum Fisher information. In general, we expect that for $s \ll x_R$ the symmetric mode is almost insensitive to small variations of s , implying $f_- > f_+ \simeq 0$. On the other hand, for $s \gg x_R$ the two sources decouple, yielding $f_+ \simeq f_-$. Although these functions are smooth, the maximum may occur in correspondence of a crossover (see Fig. 2).

Achievability: optimal states. Now we show that the upper bound established in Theorem 2 can in fact be achieved. Before presenting optimal states saturating the bound, we derive the quantum Fisher information for the case where the state of the light impinging on the image screen takes the form

$$\rho_{a_+a_-} = \sum_{n,m} p_{nm} |n, m\rangle \langle n, m|, \quad (25)$$

where $|n, m\rangle$ is a Fock state with n photons in the symmetric mode and m photons in the antisymmetric one.

The quantum Fisher information for the parameter s can be computed from $\text{QFI}_s = \text{Tr}(\mathcal{L}_s^2 \rho)$, where \mathcal{L}_s is the symmetric logarithmic derivative. For states as in Eq. (25) and given that the modes c_{\pm} emit N_{\pm} mean photons each, we obtain

$$\text{QFI}_s = \langle (\partial_s \log p)^2 \rangle + \eta N_+ \epsilon_+^2 + \eta N_- \epsilon_-^2, \quad (26)$$

where $\langle (\partial_s \log p)^2 \rangle = \sum_{nm} p_{nm} (\partial_s \log p_{nm})^2$. See Appendix C for proof. Sources as in Eq. (25) include thermal states and two-mode squeezed states, whose quantum Fisher information is computed in Appendix D.

The case of thermal states is particularly important since most natural sources of light are thermal, especially in the setting of astronomical observations. For two sources emitting N mean thermal photons each we obtain

$$\text{QFI}_s^{\text{thermal}} = 2\eta N \left[\Delta k^2 - \frac{\eta N (1 + \eta N) \gamma^2}{(1 + \eta N)^2 - \delta^2 \eta^2 N^2} \right]. \quad (27)$$

This result extends that of Ref. [10], which considered highly attenuated incoherent sources, to the case of thermal sources of any intensity. A comparison with Eq. (21) shows that thermal light is always suboptimal for estimating the separation between the sources, apart from the region $s \gg x_R$, where we obtain $\text{QFI}_s^{\text{thermal}} \simeq \eta N \Delta k^2$. An interesting regime is that of highly attenuated light ($\eta N \ll 1$) in which case we find $\text{QFI}_s^{\text{thermal}} \simeq \eta N \Delta k^2$ for all values of the separation s .

From Eq. (26) it follows that the optimal states among number-diagonal states are those maximizing $\langle (\partial_s \log p)^2 \rangle$, which incidentally is the classical Fisher information of the

probability distribution p_{nm} [40]. This observation is exploited for proving the following result.

Theorem 3 For integer $2N$, the upper bound of Theorem 2 is saturated by sources c_+ and c_- emitting the Fock state $|N_+, N_- \rangle$ with $N_+ + N_- = 2N$. In particular, the optimal state is either $|+\rangle := |2N, 0\rangle$ or $|-\rangle := |0, 2N\rangle$. In terms of the original source modes, c_1 and c_2 , these are the entangled states

$$|\pm\rangle = \frac{1}{2^N} \sum_{j=0}^{2N} \sqrt{\binom{2N}{j}} (\pm 1)^{2N-j} |j\rangle_1 |2N-j\rangle_2, \quad (28)$$

where $|k\rangle_{1,2}$ is a Fock state for $c_{1,2}$.

Proof. Since each mode c_{\pm} is independently attenuated by a attenuation factor η_{\pm} , the source state $|N_+, N_- \rangle = (N_+!N_-!)^{-1/2} (c_+^\dagger)^{N_+} (c_-^\dagger)^{N_-} |0\rangle$ is mapped into an image state of the form (25) with $p_{nm} = p_n^+ p_m^-$ and

$$p_n^{\pm} = \binom{N_{\pm}}{n} \eta_{\pm}^n (1 - \eta_{\pm})^{N_{\pm}-n}. \quad (29)$$

For such a state we obtain

$$\langle (\partial_s \log p)^2 \rangle = \langle (\partial_s \log p^+)^2 \rangle + \langle (\partial_s \log p^-)^2 \rangle \quad (30)$$

$$= \frac{\eta N_+ \gamma^2}{(1 + \delta)(1 - (1 + \delta)\eta)} + \frac{\eta N_- \gamma^2}{(1 - \delta)(1 - (1 - \delta)\eta)}. \quad (31)$$

Inserting this result into Eq. (26) we obtain that the Fock state $|N_+, N_- \rangle$ yields

$$\text{QFI}_s = \frac{\eta}{x_R^2} (N_+ f_+ + N_- f_-). \quad (32)$$

The maximum of this quantity under the constraint $N_+ + N_- = 2N$ is obtained by putting either $N_+ = 2N$ or $N_+ = 0$, hence saturating the upper bound of Theorem 3. ■

We remark that the optimal states in Theorem 3 have the same form of the optimal states for the estimation of the loss parameter of a bosonic channel [25]. Following [25], optimal states for non-integer $2N$ can be approximated by superposition of Fock states with different photon numbers. Sources emitting photons in a two-mode squeezed vacuum and sources of separable but quantum-correlated thermal light exhibits features similar to the optimal states (see Appendix D 2 and D 3).

Ultimate quantum Fisher information. Having found a matching lower bound implies that Eq. (21) is in fact achievable and represents the ultimate quantum Fisher information, optimized over the state of the light emitted by the sources. It is clear that optimal states can be explicitly engineered in all those scenarios where we can control the light emitted by the sources, which is a typical case in microscopy.

For $s \gg x_R$ the overlap δ between the image modes becomes negligible, hence Eq. (21) yields $\text{QFI}_s \simeq 2\eta N \Delta k^2 \sim$

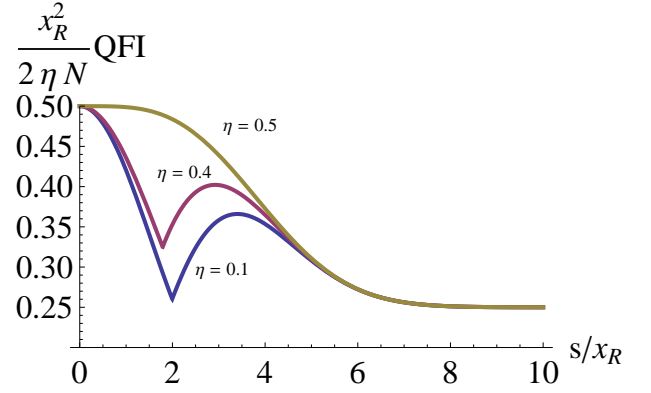


FIG. 2: Ultimate precision bound for the estimation of the separation between two point-like sources, measured in Rayleigh units. The plot shows the ultimate quantum Fisher information per photon, for a Gaussian point spread function. From bottom to top, we consider the following optical attenuation $\eta = 0.1, 0.4$, and 0.5 . The corresponding functions f_{\pm} are plotted in Fig. 3 in the Appendix.

$2\eta N x_R^{-2}$. On the other hand, for generic values of the separation s and all values of the optical attenuation η , we find $\text{QFI}_s > 2\eta N \Delta k^2$. This means that the closer the sources are the better their distance can be estimated. This counter-intuitive phenomenon is a *super-resolution* effect which appears at the sub-Rayleigh scale for entangled sources. We have also found examples of quantum-correlated sources that are not entangled (but discordant) which displays super-resolution at the sub-Rayleigh scale (see Appendix D 3).

The super-resolution is explicitly shown in the example of Fig. 2, where we consider a Gaussian point spread function $\psi(x) \sim \exp[-x^2/(4x_R^2)]$ with variance x_R^2 . In this case, $\Delta k^2 = 1/(4x_R^2)$ which yields $\lim_{s \gg x_R} \text{QFI}_s = 2\eta N \Delta k^2 = \eta N/(2x_R^2)$. Fig. 2 shows the ultimate (normalized) quantum Fisher information per photon, i.e., $x_R^2 \text{QFI}_s/(2\eta N)$, versus the dimensionless separation s/x_R . The upper bound has a maximum for finite s in the sub-Rayleigh region. The maximum value of the quantum Fisher information per photon is $1/2$ which is reached for $s/x_R \rightarrow 0$.

Optimal measurements at the sub-Rayleigh scale. We now present a sub-optimal measurement that is optimal for $s \lesssim x_R$. We consider sources emitting light in the optimal state as in Theorem 3. We also consider a standard setting where the point spread function is symmetric around its center, i.e., $\psi(x - y) = \psi(|x - y|)$. It follows that the image modes

$$a_{\pm}^{\dagger} = \frac{1}{\sqrt{2(1 \pm \delta)}} \int dx [\psi(x + s/2) \pm \psi(x - s/2)] a_x^{\dagger}, \quad (33)$$

are respectively even and odd functions of the coordinate x . We can hence consider a measurement able to distinguish the parity as, for example, photo-detection of the Hermite-Gauss modes. (This kind of measurement is optimal also in other settings [10]. See also Ref. [41] for a more general approach).

Consider photon counting in the space of even and odd functions. The probability of counting n photons in even modes is given by p_n^+ , and the probability of n photons in

odd modes is given by p_n^- . The (classical) Fisher information associated to this measurement is

$$F_s = \left\langle (\partial_s \log p^+)^2 \right\rangle + \left\langle (\partial_s \log p^-)^2 \right\rangle \quad (34)$$

$$= \frac{\eta N_+ \gamma^2}{(1+\delta)(1-(1+\delta)\eta)} + \frac{\eta N_- \gamma^2}{(1-\delta)(1-(1-\delta)\eta)}.$$

For $s \lesssim x_R$, this non-adaptive measurement is optimal for almost all values of η (but for $\eta \sim 0.5$). For larger values of s it fails to be optimal because it does not account for the fact that a change in the value of the separation s also implies a translation of the image modes on the image screen.

Conclusions. We have found the ultimate precision bound for estimating the separation between two point-like sources using a linear-optical imaging system, considering arbitrary quantum states for the sources. Although we have focused on the problem of estimating the separation between two sources, our approach can be immediately extended to the problem of estimating the location of a single source.

Our findings show that the separation between sources emitting quantum-correlated light (entangled or discordant) can be super-resolved at the sub-Rayleigh region. In particular, we have found the optimal entangled states with this

feature. Under optimal conditions one can increase the sub-Rayleigh quantum Fisher information by a constant factor with respect of its value for separations much larger than the Rayleigh length. In the sub-Rayleigh regime, we have shown that photon counting in the symmetric and antisymmetric modes is an optimal measurement.

Another consequence of our findings is that the ultimate accuracy for any linear-optical, far-field imaging system in the paraxial approximation scales according to the standard quantum limit. While in principle it could still be possible to beat the standard quantum limit, our results show that in order to do so it is necessary to rely on a biased estimator for the source separation, to consider non-point-like sources, or to employ a near-field, non-linear, or non-paraxial imaging system.

Note added. The specification of our general result of Eq. (21) to the case of thermal sources [see Eq. (27)] has been independently found by Nair and Tsang [42]; these authors also study tailored measurements that are almost optimal for estimating the separation between two thermal sources.

Acknowledgments. We thank R. Nair, M. Tsang, K. Macieszczak, G. Adesso and G. A. Durkin for their valuable comments. C.L. is also grateful to R. Accardo and L. Iorio, without whose support this work would not have been possible.

Appendix A: A set of normal modes for the field on the image plane

In the main body of the paper we define the operators

$$a_1 = \int dx \psi^*(x + s/2) a_x, \quad (A1)$$

$$a_2 = \int dx \psi^*(x - s/2) a_x, \quad (A2)$$

$$\frac{\partial a_1}{\partial s} = \int dx \frac{d\psi^*(x + s/2)}{ds} a_x, \quad (A3)$$

$$\frac{\partial a_2}{\partial s} = \int dx \frac{d\psi^*(x - s/2)}{ds} a_x, \quad (A4)$$

where a_x, a_x^\dagger are the canonical creation and annihilation operators for the field at location x on the image screen.

The operators $a_1, a_2, \frac{\partial a_1}{\partial s}, \frac{\partial a_2}{\partial s}$ do not define a set of canonical bosonic modes. Following [10], we define the operators a_+, a_-, b_+, b_- as:

$$a_- = \frac{a_1 - a_2}{\sqrt{2(1-\delta)}}, \quad (A5)$$

$$a_+ = \frac{a_1 + a_2}{\sqrt{2(1+\delta)}}, \quad (A6)$$

$$b_- = -\frac{\sqrt{2}}{\epsilon_-} \left[\frac{\partial a_1}{\partial s} - \frac{\partial a_2}{\partial s} + \frac{\gamma}{\sqrt{2(1-\delta)}} a_- \right], \quad (A7)$$

$$b_+ = -\frac{\sqrt{2}}{\epsilon_+} \left[\frac{\partial a_1}{\partial s} + \frac{\partial a_2}{\partial s} - \frac{\gamma}{\sqrt{2(1+\delta)}} a_+ \right], \quad (A8)$$

with

$$\delta = \text{Re} \int dx \psi^*(x + s/2) \psi(x - s/2), \quad (\text{A9})$$

$$\epsilon_-^2 = \Delta k^2 + \beta - \frac{\gamma^2}{1 - \delta}, \quad (\text{A10})$$

$$\epsilon_+^2 = \Delta k^2 - \beta - \frac{\gamma^2}{1 + \delta}, \quad (\text{A11})$$

$$\beta = \int dx \frac{d\psi(x + s/2)}{dx} \frac{d\psi(x - s/2)}{dx}, \quad (\text{A12})$$

$$\Delta k^2 = \int dx \left| \frac{d\psi(x)}{dx} \right|^2, \quad (\text{A13})$$

$$\gamma = \int dx \frac{d\psi(x)}{dx} \psi(x - s) = \frac{d\delta}{ds}. \quad (\text{A14})$$

The modes a_+ , a_- , b_+ , b_- satisfy canonical commutation relations under the condition that the phase of the point-spread function ψ is constant, which is the case up to corrections of the second order in the paraxial approximation [19]. In any case, as noted in [10], a possible residual phase can be locally compensated.

In terms of the canonical operators a_\pm , b_\pm we then obtain

$$\frac{\partial a_1}{\partial s} \pm \frac{\partial a_2}{\partial s} = -\frac{\epsilon_\pm}{\sqrt{2}} b_\pm \pm \frac{\gamma}{\sqrt{2(1 \pm \delta)}} a_\pm, \quad (\text{A15})$$

and

$$\frac{\partial a_\pm}{\partial s} = -\frac{\epsilon_\pm}{2\sqrt{1 \pm \delta}} b_\pm. \quad (\text{A16})$$

Appendix B: Variance of the effective beam-splitter Hamiltonian

In this Section we compute the variance

$$\langle \psi' | \Delta^2 H^{\text{eff}} | \psi' \rangle = \langle \psi' | (H^{\text{eff}})^2 | \psi' \rangle - \langle \psi' | H^{\text{eff}} | \psi' \rangle^2 \quad (\text{B1})$$

$$= \langle \psi' | (\omega_+ H_+^{\text{eff}} + \omega_- H_-^{\text{eff}})^2 | \psi' \rangle - (\langle \psi' | \omega_+ H_+^{\text{eff}} + \omega_- H_-^{\text{eff}} | \psi' \rangle)^2, \quad (\text{B2})$$

where

$$|\psi'\rangle = (e^{-i\theta_+ H_+} e^{-i\theta_- H_-} |\psi\rangle_{c_+ c_-} |0\rangle_{v_+ v_-}) |0\rangle_{b_+ b_-}. \quad (\text{B3})$$

is the state of the light at the image screen, together with the state of the auxiliary modes v_\pm , b_\pm .

Here

$$H_\pm = i \left(c_\pm^\dagger v_\pm - v_\pm^\dagger c_\pm \right), \quad (\text{B4})$$

and

$$H^{\text{eff}} = \omega_+ H_+^{\text{eff}} + \omega_- H_-^{\text{eff}}, \quad (\text{B5})$$

with

$$\omega_\pm H_\pm^{\text{eff}} = i A_\pm \left(c_\pm^\dagger v_\pm - c_\pm v_\pm^\dagger \right) + i B_\pm \left(c_\pm^\dagger b_\pm - c_\pm^\dagger b_\pm \right), \quad (\text{B6})$$

and $A_\pm = \frac{d\theta_\pm}{ds}$, $B_\pm = \frac{\epsilon_\pm}{2\sqrt{1 \pm \delta}}$.

We then obtain

$$\begin{aligned} \langle \psi' | \Delta^2 H^{\text{eff}} | \psi' \rangle &= \langle \psi' | \left[i A_+ \left(c_+^\dagger v_+ - c_+ v_+^\dagger \right) + i A_- \left(c_-^\dagger v_- - c_- v_-^\dagger \right) \right. \\ &\quad \left. + i B_+ \left(c_+^\dagger b_+ - c_+ b_+^\dagger \right) + i B_- \left(c_-^\dagger b_- - c_- b_-^\dagger \right) \right]^2 | \psi' \rangle \\ &\quad - \langle \psi' | \left[i A_+ \left(c_+^\dagger v_+ - c_+ v_+^\dagger \right) + i A_- \left(c_-^\dagger v_- - c_- v_-^\dagger \right) \right. \\ &\quad \left. + i B_+ \left(c_+^\dagger b_+ - c_+ b_+^\dagger \right) + i B_- \left(c_-^\dagger b_- - c_- b_-^\dagger \right) \right] | \psi' \rangle^2. \end{aligned} \quad (\text{B7})$$

It follows from (B3) that $b_{\pm}|\psi'\rangle = 0$, which implies

$$\begin{aligned} \langle\psi'|\Delta^2 H^{\text{eff}}|\psi'\rangle &= \langle\psi'| \left[iA_+ \left(c_+^\dagger v_+ - c_+ v_+^\dagger \right) + iA_- \left(c_-^\dagger v_- - c_- v_-^\dagger \right) \right]^2 |\psi'\rangle \\ &\quad + \langle\psi'| \left[iB_+ \left(c_+^\dagger b_+ - c_+ b_+^\dagger \right) + iB_- \left(c_-^\dagger b_- - c_- b_-^\dagger \right) \right]^2 |\psi'\rangle \\ &\quad - \langle\psi'| \left[iA_+ \left(c_+^\dagger v_+ - c_+ v_+^\dagger \right) + iA_- \left(c_-^\dagger v_- - c_- v_-^\dagger \right) \right] |\psi'\rangle^2 \end{aligned} \quad (\text{B8})$$

$$\begin{aligned} &= \langle\psi'| \left[iA_+ \left(c_+^\dagger v_+ - c_+ v_+^\dagger \right) + iA_- \left(c_-^\dagger v_- - c_- v_-^\dagger \right) \right]^2 |\psi'\rangle \\ &\quad + \langle\psi'| \left(B_+^2 c_+^\dagger c_+ + B_-^2 c_-^\dagger c_- \right) |\psi'\rangle \\ &\quad - \langle\psi'| \left[iA_+ \left(c_+^\dagger v_+ - c_+ v_+^\dagger \right) + iA_- \left(c_-^\dagger v_- - c_- v_-^\dagger \right) \right] |\psi'\rangle^2. \end{aligned} \quad (\text{B9})$$

Since the operator $iA_+ \left(c_+^\dagger v_+ - c_+ v_+^\dagger \right) + iA_- \left(c_-^\dagger v_- - c_- v_-^\dagger \right)$ commutes with the Hamiltonian $H_+ + H_-$, its expectation values on $|\psi'\rangle = (e^{-i\theta_+ H_+} e^{-i\theta_- H_-} |\psi\rangle_{c_+ c_-} |0\rangle_{v_+ v_-}) |0\rangle_{b_+ b_-}$ equal the expectations values on $|\psi, 0\rangle := |\psi\rangle_{c_+ c_-} |0\rangle_{v_+ v_-}$, which implies

$$\begin{aligned} \langle\psi'|\Delta^2 H^{\text{eff}}|\psi'\rangle &= \langle\psi, 0| \left[iA_+ \left(c_+^\dagger v_+ - c_+ v_+^\dagger \right) + iA_- \left(c_-^\dagger v_- - c_- v_-^\dagger \right) \right]^2 |\psi, 0\rangle \\ &\quad + \langle\psi'| \left(B_+^2 c_+^\dagger c_+ + B_-^2 c_-^\dagger c_- \right) |\psi'\rangle \\ &\quad - \langle\psi, 0| \left[iA_+ \left(c_+^\dagger v_+ - c_+ v_+^\dagger \right) + iA_- \left(c_-^\dagger v_- - c_- v_-^\dagger \right) \right] |\psi, 0\rangle^2 \end{aligned} \quad (\text{B10})$$

$$= \langle\psi, 0| \left(A_+^2 c_+^\dagger c_+ + A_-^2 c_-^\dagger c_- \right) |\psi, 0\rangle + \langle\psi'| \left(B_+^2 c_+^\dagger c_+ + B_-^2 c_-^\dagger c_- \right) |\psi'\rangle, \quad (\text{B11})$$

that is,

$$\begin{aligned} \langle\psi'|\Delta^2 H^{\text{eff}}|\psi'\rangle &= \left(\frac{d\theta_+}{ds} \right)^2 \langle\psi|c_+^\dagger c_+|\psi\rangle + \frac{\epsilon_+^2}{4(1+\delta)} \langle\psi'|c_+^\dagger c_+|\psi'\rangle \\ &\quad + \left(\frac{d\theta_-}{ds} \right)^2 \langle\psi|c_-^\dagger c_-|\psi\rangle + \frac{\epsilon_-^2}{4(1-\delta)} \langle\psi'|c_-^\dagger c_-|\psi'\rangle. \end{aligned} \quad (\text{B12})$$

It is important to remark that in this last expression for the variance $\langle\psi'|\Delta^2 H^{\text{eff}}|\psi'\rangle$, there are no cross-terms coupling the operators c_+ , c_+^\dagger with the operators c_- , c_-^\dagger . This implies that the upper bound on the quantum Fisher information is the sum of two independent terms.

Assume that the source c_{\pm} emits N_{\pm} mean photons, that is, $\langle\psi|c_{\pm}^\dagger c_{\pm}|\psi\rangle = N_{\pm}$, which in turn implies $\langle\psi'|c_{\pm}^\dagger c_{\pm}|\psi'\rangle = \eta_{\pm} N_{\pm} = (1 \pm \delta) \eta N_{\pm}$. Then we obtain the following upper bound on the quantum Fisher information:

$$\text{QFI}_s \leq 4N_+ \left[\left(\frac{d\theta_+}{ds} \right)^2 + \frac{\eta \epsilon_+^2}{4} \right] + 4N_- \left[\left(\frac{d\theta_-}{ds} \right)^2 + \frac{\eta \epsilon_-^2}{4} \right] \quad (\text{B13})$$

$$= N_+ \left[\frac{\eta \gamma^2}{(1+\delta)(1-(1+\delta)\eta)} + \eta \epsilon_+^2 \right] + N_- \left[\frac{\eta \gamma^2}{(1-\delta)(1-(1-\delta)\eta)} + \eta \epsilon_-^2 \right]. \quad (\text{B14})$$

Given a constraint of $N_+ + N_- = 2N$ total mean photons emitted by the sources, the maximum of the right hand side is obtained putting either $N_+ = 2N$ and $N_- = 0$ or $N_+ = 0$ and $N_- = 2N$. We then obtain

$$\text{QFI}_s \leq 2\eta N \max \left\{ \frac{\gamma^2}{(1+\delta)(1-(1+\delta)\eta)} + \epsilon_+^2, \frac{\gamma^2}{(1-\delta)(1-(1-\delta)\eta)} + \epsilon_-^2 \right\}. \quad (\text{B15})$$

As an example, consider the case of a Gaussian point-spread function, $\psi(x) \sim \exp \left(-\frac{x^2}{4x_R^2} \right)$. The quantities

$$f_+ := x_R^2 \left[\frac{\gamma^2}{(1+\delta)(1-(1+\delta)\eta)} + \epsilon_+^2 \right] \quad (\text{B16})$$

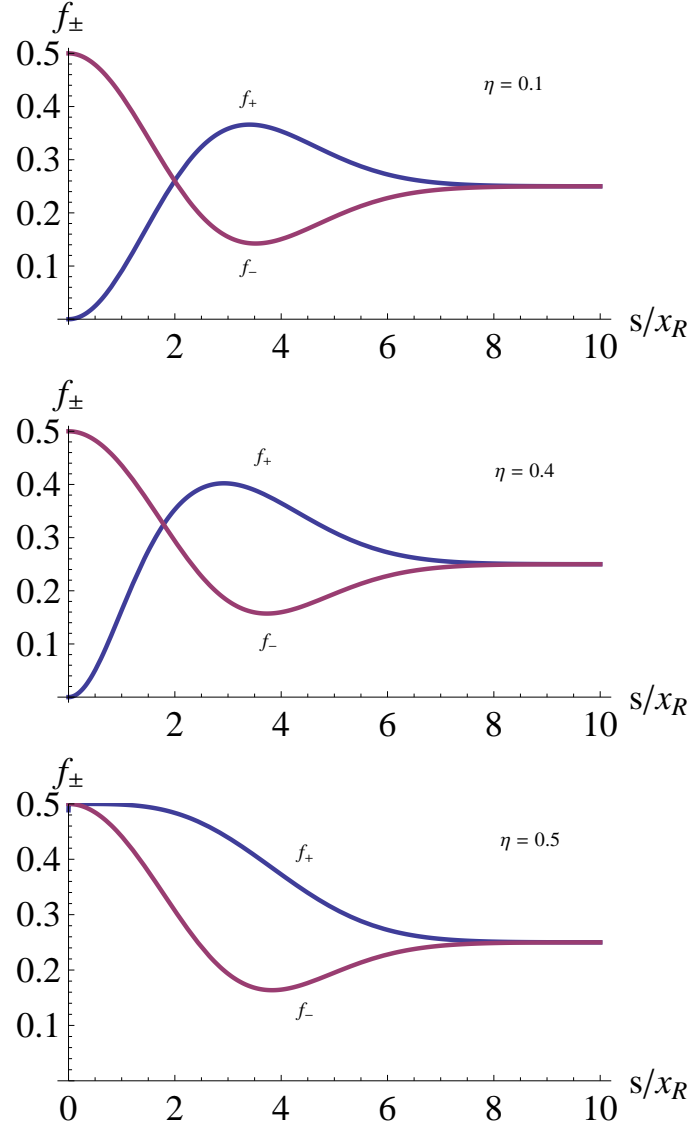


FIG. 3: The quantities f_{\pm} defined in Eqs. (B16)-(B17) plotted versus the separation s/x_R for different values of η . From top to bottom, $\eta = 0.1, 0.4, 0.5$.

and

$$f_- := x_R^2 \left[\frac{\gamma^2}{(1-\delta)(1-(1-\delta)\eta)} + \epsilon_-^2 \right] \quad (\text{B17})$$

are plotted versus the s/x_R in Fig. 3 for different values of η . As the figures show, which is the maximum between f_+ and f_- depend both on η and s .

Appendix C: Quantum Fisher information for number-diagonal states

In this section we compute the quantum Fisher information for number-diagonal states of the form

$$\rho_{a_+ a_-} = \sum_{n,m} p_{nm} |n; m\rangle \langle n; m|, \quad (\text{C1})$$

where $|n; m\rangle = (n!m!)^{-1/2} a_+^\dagger{}^n a_-^\dagger{}^m |0\rangle$ denotes a Fock state with n photons in the symmetric mode and m photons in the anti-symmetric one.

The quantum Fisher information for the parameter s can be computed by applying the formula $\text{QFI}_s = \text{Tr}(\mathcal{L}_s^2 \rho)$, where

$$\mathcal{L}_s = \sum_{n,n',m,m' | p_{nm} + p_{n'm'} > 0} \left(\frac{2}{p_{nm} + p_{n'm'}} \right) |n; m\rangle \langle n; m| \frac{\partial \rho}{\partial s} |n'; m'\rangle \langle n'; m'| \quad (\text{C2})$$

is the symmetric logarithmic derivative.

The derivative of ρ with respect to s reads

$$\partial_s \rho = \sum_{n,m} (\partial_s p_{nm}) |n; m\rangle \langle n; m| + p_{nm} \partial_s (|n; m\rangle \langle n; m|) \quad (\text{C3})$$

$$= \sum_{n,m} (\partial_s p_{nm}) |n; m\rangle \langle n; m| + p_{nm} \partial_s \left(\frac{a_+^\dagger{}^n}{\sqrt{n!}} \frac{a_-^\dagger{}^m}{\sqrt{m!}} |0\rangle \langle 0| \frac{a_+^n}{\sqrt{n!}} \frac{a_-^m}{\sqrt{m!}} \right) \quad (\text{C4})$$

$$= \sum_{n,m} (\partial_s p_{nm}) |n; m\rangle \langle n; m| + p_{nm} \frac{n}{\sqrt{n!}} \frac{\partial a_+^\dagger}{\partial s} a_+^{\dagger n-1} |0; m\rangle \langle n; m| + p_{nm} \frac{n}{\sqrt{n!}} |n; m\rangle \langle 0; m| a_+^{n-1} \frac{\partial a_+}{\partial s} + p_{nm} \frac{m}{\sqrt{m!}} \frac{\partial a_-^\dagger}{\partial s} a_-^{\dagger m-1} |n; 0\rangle \langle n; m| + p_{nm} \frac{m}{\sqrt{m!}} |n; m\rangle \langle n; 0| a_-^{m-1} \frac{\partial a_-}{\partial s} \quad (\text{C5})$$

$$= \sum_{n,m} (\partial_s p_{nm}) |n; m\rangle \langle n; m| + p_{nm} \sqrt{n} \left(\frac{\partial a_+^\dagger}{\partial s} |n-1; m\rangle \langle n; m| + |n; m\rangle \langle n-1; m| \frac{\partial a_+}{\partial s} \right) + p_{nm} \sqrt{m} \left(\frac{\partial a_-^\dagger}{\partial s} |n; m-1\rangle \langle n; m| + |n; m\rangle \langle n; m-1| \frac{\partial a_-}{\partial s} \right). \quad (\text{C6})$$

Now we apply Eq. (A16). Putting $|n-1, 1; m\rangle = b_+^\dagger |n-1; m\rangle$ and $|n; m-1, 1\rangle = b_-^\dagger |n; m-1\rangle$ we obtain

$$\begin{aligned} \partial_s \rho = & \sum_{n,m} (\partial_s p_{nm}) |n; m\rangle \langle n; m| \\ & - \frac{p_{nm} \sqrt{n} \epsilon_+}{2\sqrt{1+\delta}} (|n-1, 1; m\rangle \langle n; m| + |n; m\rangle \langle n-1, 1; m|) \\ & - \frac{p_{nm} \sqrt{m} \epsilon_-}{2\sqrt{1-\delta}} (|n; m-1, 1\rangle \langle n; m| + |n; m\rangle \langle n; m-1, 1|), \end{aligned} \quad (\text{C7})$$

from which we compute the symmetric logarithmic derivative

$$\begin{aligned} \mathcal{L}_s = & \sum_{n,m} (\partial_s \log p_{nm}) |n; m\rangle \langle n; m| \\ & - \frac{\sqrt{n} \epsilon_+}{\sqrt{1+\delta}} (|n-1, 1; m\rangle \langle n; m| + |n; m\rangle \langle n-1, 1; m|) \\ & - \frac{\sqrt{m} \epsilon_-}{\sqrt{1-\delta}} (|n; m-1, 1\rangle \langle n; m| + |n; m\rangle \langle n; m-1, 1|). \end{aligned} \quad (\text{C8})$$

Assuming that each source mode c_\pm emits N_\pm mean photons, then the quantum Fisher information reads

$$\text{QFI}_s = \langle (\partial_s \log p)^2 \rangle + \eta N_+ \epsilon_+^2 + \eta N_- \epsilon_-^2, \quad (\text{C9})$$

with $\langle (\partial_s \log p)^2 \rangle = \sum_{nm} p_{nm} (\partial_s \log p_{nm})^2$.

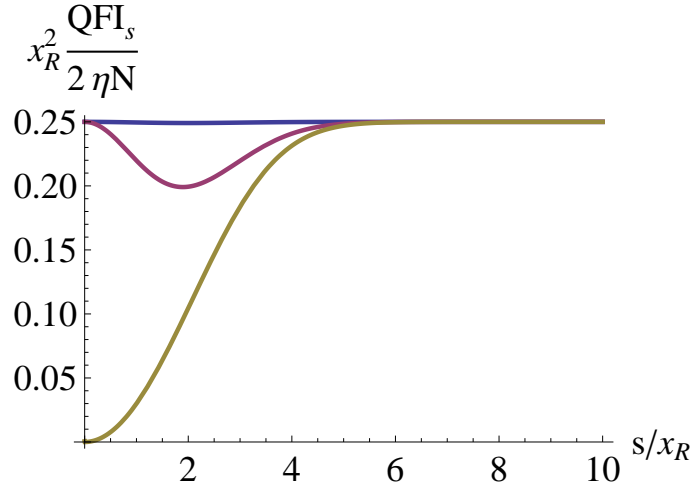


FIG. 4: Quantum Fisher information for the estimation of the separation between two point-like sources emitting thermal light. The plot shows the quantum Fisher information per photon for a Gaussian point-spread function with variance x_R^2 . From top to bottom $\eta N = 0.01, 1$ and the semiclassical limit $\eta N \rightarrow \infty$.

Appendix D: Special cases: thermal, correlated, and squeezed sources

1. Thermal sources

Let us first assume that the modes c_1, c_2 emit thermal monochromatic light at a given temperature, with N mean photons each, then the modes c_{\pm} will be thermal too and at the same temperature. It follows that the modes a_{\pm} on the image screen are also thermal, but with mean photons $M_{\pm} = \eta(1 \pm \delta)N$, respectively.

The state of the two image modes has the form

$$\rho_{a_+ a_-} = \frac{1}{M_+ + 1} \frac{1}{M_- + 1} \sum_{n,m} \left(\frac{M_+}{M_+ + 1} \right)^n \left(\frac{M_-}{M_- + 1} \right)^m |n; m\rangle \langle n; m|. \quad (\text{D1})$$

Since this is a number-diagonal state as in Eq. (C1), we can apply Eq. (C9). A straightforward calculation then yields

$$\langle (\partial_s \log p)^2 \rangle = 2\eta N \left[\frac{\gamma^2}{2(1+\delta)(1+(1+\delta)\eta N)} + \frac{\gamma^2}{2(1-\delta)(1+(1-\delta)\eta N)} \right], \quad (\text{D2})$$

and

$$\text{QFI}_s = \langle (\partial_s \log p)^2 \rangle + 2\eta N \left[\Delta k^2 - \frac{\gamma^2}{2(1+\delta)} - \frac{\gamma^2}{2(1-\delta)} \right] \quad (\text{D3})$$

$$= 2\eta N \left[\frac{\gamma^2}{2(1+\delta)(1+(1+\delta)\eta N)} + \frac{\gamma^2}{2(1-\delta)(1+(1-\delta)\eta N)} \right] + 2\eta N \left[\Delta k^2 - \frac{\gamma^2}{2(1+\delta)} - \frac{\gamma^2}{2(1-\delta)} \right] \quad (\text{D4})$$

$$= 2\eta N \left[\Delta k^2 - \frac{\eta N(1+\eta N)\gamma^2}{(1+\eta N)^2 - \delta^2 \eta^2 N^2} \right]. \quad (\text{D5})$$

In the semiclassical limit, $\eta N \gg 1$, the quantum Fisher information per photon reads $\lim_{\eta N \gg 1} \text{QFI}_s / (2\eta N) = \Delta k^2 - \frac{\gamma^2}{2(1+\delta)} - \frac{\gamma^2}{2(1-\delta)}$. As an example, consider the Gaussian point-spread function, $\psi(x) \sim \exp\left(-\frac{x^2}{4x_R^2}\right)$. This is shown in Fig. 4, where one can see that for bright thermal sources the quantum Fisher information vanishes for $s \ll x_R$ — a typical classical feature dubbed the “Rayleigh’s curse” in [10]. We note that the same result for thermal sources has been independently obtained by [42].

2. Two-mode squeezed sources

We now consider the case of two sources emitting a continuous-variable quadrature-entangled state (two-mode squeezed vacuum) of the form [35, 36]

$$|\xi\rangle = \exp\left[\xi\left(c_1^\dagger c_2^\dagger - c_1 c_2\right)\right]|0\rangle. \quad (\text{D6})$$

In terms of the modes c_\pm , this reads

$$|\xi\rangle = \exp\left[\frac{\xi}{2}\left(c_+^{\dagger 2} - c_+^2\right)\right] \otimes \exp\left[-\frac{\xi}{2}\left(c_-^{\dagger 2} - c_-^2\right)\right]|0\rangle, \quad (\text{D7})$$

which describes the direct product of two independent squeezed vacua [35, 36]. Each of these modes is independently attenuated when it enters the optical imaging system, that is, the state of the modes a_\pm on the image screen is that of two independent attenuated squeezed vacua.

To describe these states it is convenient to use the covariance matrix of the quadrature operators, $X_\pm = (c_\pm + c_\pm^\dagger)/\sqrt{2}$ and $P_\pm = -i(c_\pm - c_\pm^\dagger)/\sqrt{2}$. In our case the first moments of the quadrature operators vanish, and the covariance matrix reads

$$V_{c_+, c_-} = \langle \xi | \left(\begin{array}{cc} X_+^2 & \frac{X_+ P_+ + P_+ X_+}{2} \\ \frac{X_+ P_+ + P_+ X_+}{2} & P_+^2 \end{array} \right) \oplus \left(\begin{array}{cc} X_-^2 & \frac{X_- P_- + P_- X_-}{2} \\ \frac{X_- P_- + P_- X_-}{2} & P_-^2 \end{array} \right) | \xi \rangle \quad (\text{D8})$$

$$= \left(\begin{array}{cc} \frac{1}{2} e^{2\xi} & 0 \\ 0 & \frac{1}{2} e^{-2\xi} \end{array} \right) \oplus \left(\begin{array}{cc} \frac{1}{2} e^{-2\xi} & 0 \\ 0 & \frac{1}{2} e^{2\xi} \end{array} \right). \quad (\text{D9})$$

The covariance matrix describing the image modes is obtained by attenuating the modes by factors $\eta_\pm = (1 \pm \delta)\eta$:

$$V_{a_+, a_-} = \left(\begin{array}{cc} \frac{\eta_+}{2} e^{2\xi} + \frac{1-\eta_+}{2} & 0 \\ 0 & \frac{\eta_+}{2} e^{-2\xi} + \frac{1-\eta_+}{2} \end{array} \right) \oplus \left(\begin{array}{cc} \frac{\eta_-}{2} e^{-2\xi} + \frac{1-\eta_-}{2} & 0 \\ 0 & \frac{\eta_-}{2} e^{2\xi} + \frac{1-\eta_-}{2} \end{array} \right). \quad (\text{D10})$$

We can re-parameterize this covariance matrix in terms of the variables T_\pm, r_\pm as

$$V_{a_+, a_-} = \left(\begin{array}{cc} e^{2r_+} \left(T_+ + \frac{1}{2}\right) & 0 \\ 0 & e^{-2r_+} \left(T_+ + \frac{1}{2}\right) \end{array} \right) \oplus \left(\begin{array}{cc} e^{-2r_-} \left(T_- + \frac{1}{2}\right) & 0 \\ 0 & e^{2r_-} \left(T_- + \frac{1}{2}\right) \end{array} \right), \quad (\text{D11})$$

with

$$T_\pm = \frac{1}{2} \left(\sqrt{\eta_\pm^2 + (1 - \eta_\pm)^2 + 2\eta_\pm(1 - \eta_\pm) \cosh(2\xi)} - 1 \right) \quad (\text{D12})$$

and

$$r_\pm = \frac{1}{2} \sinh^{-1} \left(\frac{\eta_\pm \sinh(2\xi)}{2T_\pm + 1} \right). \quad (\text{D13})$$

Using this parameterization, the state of each image mode is described as being the result of applying a squeezing transformation to a thermal state. That is, the state of the modes a_+, a_- has the form.

$$\rho_{a_+ a_-} = \rho_+ \otimes \rho_- , \quad (\text{D14})$$

where

$$\rho_\pm = \frac{1}{T_\pm + 1} \sum_{n=0}^{\infty} \left(\frac{T_\pm}{T_\pm + 1} \right)^n |e_n\rangle_\pm \langle e_n| = \sum_{n=0}^{\infty} p_n^\pm |e_n\rangle_\pm \langle e_n| \quad (\text{D15})$$

and

$$|e_n\rangle_\pm = e^{-iK_\pm} |n\rangle_\pm = \exp\left[\pm \frac{r_\pm}{2} \left(a_\pm^{\dagger 2} - a_\pm^2\right)\right] |n\rangle_\pm \quad (\text{D16})$$

is a squeezed n -photon Fock state.

Therefore, the state $\rho_{a_+a_-}$ is not diagonal in the number basis, but in the basis $\{|e_n\rangle_\pm\}$ that is unitarily related to the latter by the action of the unitary e^{-iK_\pm} . The derivative of ρ_\pm with respect to s reads

$$\partial_s \rho_\pm = \sum_n (\partial_s p_n^\pm) |e_n\rangle_\pm \langle e_n| + p_n^\pm \partial_s (|e_n\rangle_\pm \langle e_n|) \quad (\text{D17})$$

$$= \sum_n (\partial_s p_n^\pm) |e_n\rangle_\pm \langle e_n| + p_n^\pm e^{-iK_\pm} \partial_s (|n\rangle_\pm \langle n|) e^{iK_\pm} + p_n^\pm [\partial_s (e^{-iK_\pm}) |n\rangle_\pm \langle e_n| + |e_n\rangle_\pm \langle n| \partial_s (e^{iK_\pm})] . \quad (\text{D18})$$

Comparing with (C3), now we have one extra term accounting for the derivative of e^{-iK_\pm} with respect to s . From the Baker–Campbell–Hausdorff formula we obtain

$$e^{iK_\pm} \partial_s e^{-iK_\pm} = -iA_\pm K_\pm + \frac{B_\pm}{2} (a_\pm^\dagger b_\pm^\dagger - a_\pm b_\pm) \sinh r_\pm + \frac{B_\pm}{2} (a_\pm^\dagger b_\pm - a_\pm b_\pm^\dagger) (\cosh r_\pm - 1) , \quad (\text{D19})$$

with

$$A_\pm = \frac{\partial \log r_\pm}{\partial s} \quad (\text{D20})$$

and

$$B_\pm = \frac{\epsilon_\pm}{\sqrt{1 \pm \delta}} . \quad (\text{D21})$$

This allows us to compute the quantum Fisher information. We obtain:

$$\begin{aligned} \text{QFI}_s = & \left\langle \left(\frac{\partial \log p^+}{\partial s} \right)^2 \right\rangle + \left\langle \left(\frac{\partial \log p^-}{\partial s} \right)^2 \right\rangle \\ & + \eta (\cosh 2\xi - 1) \left(\Delta k^2 - \frac{\gamma^2}{2(1+\delta)} - \frac{\gamma^2}{2(1-\delta)} \right) \\ & + \frac{2(2T_+ + 1)^2}{2T_+^2 + 2T_+ + 1} \frac{\partial r_+}{\partial s} + \frac{2(2T_- + 1)^2}{2T_-^2 + 2T_- + 1} \frac{\partial r_-}{\partial s} . \end{aligned}$$

For $s \gg 1$ we have $\text{QFI}_s \simeq \eta (\cosh 2\xi - 1) \Delta k^2$, where $\eta (\cosh 2\xi - 1)$ is the mean photon number impinging on the image screen.

As an example, Fig. 5 shows the quantum Fisher information per photon impinging on the image screen versus s/\times_R , for the Gaussian point-spread function. For small values of η the light is highly attenuated and we observed the same behavior as highly attenuated incoherent sources, while for small η and relatively large squeezing ξ the state becomes effectively semiclassical and manifests the classical ‘‘Rayleigh’s curse’’ [10]. On the other hand, for larger value of η we observe a phenomenon of super-resolution for sub-Rayleigh distances, similarly to the optimal entangled sources obtained in the main body of this paper.

3. Correlated thermal sources

Let us considered two sources c_1, c_2 emitting light in a Gaussian state with zero mean and covariance matrix

$$V_{c_1, c_2} = \begin{pmatrix} N + \frac{1}{2} & 0 & wN & 0 \\ 0 & N + \frac{1}{2} & 0 & wN \\ wN & 0 & N + \frac{1}{2} & 0 \\ 0 & wN & 0 & N + \frac{1}{2} \end{pmatrix} . \quad (\text{D22})$$

For $w \leq 1$, this is a correlated thermal state. Such a state is always separable but has non-zero discord. Its quantum discord can be computed exactly according to the results of Ref. [37], and it coincides with its Gaussian discord [38, 39].

Expressing the state in terms of the non-local source modes c_+ and c_- , the covariance matrix reads

$$V_{c_+, c_-} = \begin{pmatrix} N_+ + \frac{1}{2} & 0 & 0 & 0 \\ 0 & N_+ + \frac{1}{2} & 0 & 0 \\ 0 & 0 & N_- + \frac{1}{2} & 0 \\ 0 & 0 & 0 & N_- + \frac{1}{2} \end{pmatrix} , \quad (\text{D23})$$

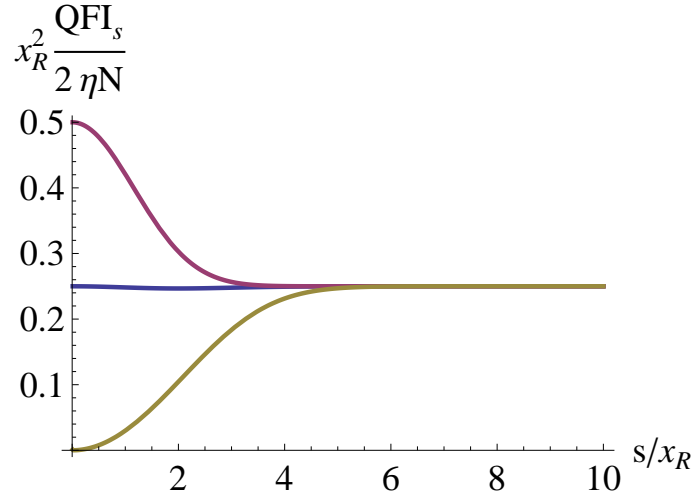


FIG. 5: Quantum Fisher information for the estimation of the separation s between two entangled sources emitting a two-mode squeezed vacuum state. The plot shows the quantum Fisher information per photon impinging on the image screen for the case of a Gaussian point-spread function with variance x_R^2 . From top to bottom: $\xi = 0.1, \eta = 0.5$; $\xi = 1, \eta = 0.01$; $\xi = 10, \eta = 0.1$.

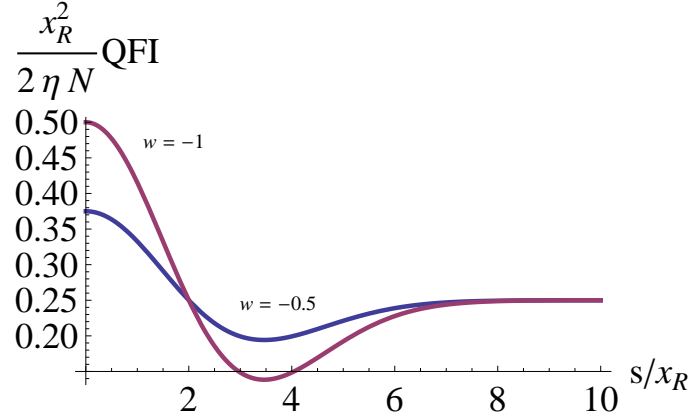


FIG. 6: Quantum Fisher information for the estimation versus the separation for sources emitting a two-mode correlated thermal state, for $w = -0.5$ and $w = -1$. These correlated sources allow for super-resolution at the sub-Rayleigh scale.

which represents the product of two thermal states with different mean photon number $N_+ = (1 + w)N$ and $N_- = (1 - w)N$.

To compute the quantum Fisher information associated to these sources, we can proceed as we have done in Section D for the case of thermal sources emitting the same mean photons. We then obtain

$$\text{QFI}_s = \eta N_+ \left[\delta k^2 - \beta - \frac{\eta N_+ \gamma^2}{1 + (1 + \delta)\eta N_+} \right] + \eta N_- \left[\delta k^2 + \beta - \frac{\eta N_- \gamma^2}{1 + (1 - \delta)\eta N_-} \right]. \quad (\text{D24})$$

As an example, let us consider the regime of highly attenuated light, $\eta N_{\pm} \ll 1$. In this limit the quantum Fisher information reads

$$\text{QFI}_s \simeq \eta N_+ (\delta k^2 - \beta) + \eta N_- (\delta k^2 + \beta) = 2\eta N (\delta k^2 - w\beta) \quad (\text{D25})$$

and yields a phenomenon of super-resolution for same value of w . For example, Fig. 6 shows the quantum Fisher information versus the separation for the case of a Gaussian point spread function, yielding super-resolution for $w < 0$.

- [3] V. Giovannetti, S. Lloyd, L. Maccone, and J. H. Shapiro, Phys. Rev. A **79**, 013827 (2009).
- [4] M. Tsang, Phys. Rev. Lett. **102**, 253601 (2009).
- [5] H. Shin, K. W. C. Chan, H. J. Chang, and R. W. Boyd, Phys. Rev. Lett. **107**, 083603 (2011).
- [6] O. Schwartz and D. Oron, Phys. Rev. A **85**, 033812 (2012).
- [7] J.-M. Cui, F.-W. Sun, X.-D. Chen, Z.-J. Gong, and G.-C. Guo, Phys. Rev. Lett. **110**, 153901 (2013).
- [8] O. Schwartz, J. M. Levitt, R. Tenne, S. Itzhakov, Z. Deutsch, and D. Oron, Nano Letters **13**, 5832 (2013).
- [9] D. Gatto Monticone, K. Katamadze, P. Traina, E. Moreva, J. Forneris, I. Ruo-Berchera, P. Olivero, I. P. Degiovanni, G. Brida, and M. Genovese, Phys. Rev. Lett. **113**, 143602 (2014).
- [10] M. Tsang, R. Nair, X. Lu, Phys. Rev. X **6**, 031033 (2016).
- [11] S. L. Braunstein, Phys. Rev. Lett. **69**, 3598 (1992).
- [12] S. L. Braunstein, and C. M. Caves, Phys. Rev. Lett. **72**, 3439 (1994).
- [13] S. L. Braunstein, C. M. Caves, and G. J. Milburn, Ann. Phys. **247**, 135 (1996).
- [14] A. N. Boto, P. Kok, D. S. Abrams, S. L. Braunstein, C. P. Williams, and J. P. Dowling, Phys. Rev. Lett. **85**, 2733 (2000).
- [15] V. Giovannetti, S. Lloyd, and L. Maccone, Science **306**, 1330 (2004).
- [16] M. G. A. Paris, International Journal of Quantum Information **7**, 125 (2009).
- [17] U. Dorner, R. Demkowicz-Dobrzanski, B. J. Smith, J. S. Lundeen, W. Wasilewski, K. Banaszek, and I. A. Walmsley, Phys. Rev. Lett. **102**, 040403 (2009).
- [18] V. Giovannetti, S. Lloyd, and L. Maccone, Nature Photonics **5**, 222 (2011).
- [19] J. W. Goodman, *Introduction to Fourier Optics* (McGraw-Hill, New York, 1968).
- [20] Z. S. Tang, K. Durak, and A. Ling, *Fault-tolerant and finite-error localization for point emitters within the diffraction limit*, arXiv: 1605.07297 (2016).
- [21] F. Yang, A. Taschilina, E. S. Moiseev, C. Simon, A. I. Lvovsky, *Far-field linear optical superresolution via heterodyne detection in a higher-order local oscillator mode*, arXiv: 1606.02662 (2016).
- [22] W.-K. Tham, H. Ferretti, A. M. Steinberg, *Beating Rayleigh's Curse by Imaging Using Phase Information*, arXiv: 1606.02666 (2016).
- [23] M. Paúr, B. Stoklasa, Z. Hradil, L. L. Sánchez-Soto, and J. Rehacek, *Achieving quantum-limited optical resolution*, arXiv: 1606.08332 (2016).
- [24] A. Monras, and M. G. A. Paris, Phys. Rev. Lett. **98**, 160401 (2007).
- [25] G. Adesso, F. Dell'Anno, S. De Siena, F. Illuminati, and L. A. M. Souza, Phys. Rev. A **79**, 040305(R) (2009).
- [26] O. Pinel, P. Jian, N. Treps, C. Fabre, and D. Braun, Phys. Rev. A **88**, 040102 (2013).
- [27] H. Venzl and M. Freyberger, Phys. Rev. A **75**, 042322 (2007).
- [28] R. Gaiba and M. G. A. Paris, Phys. Lett. A **373**, 934 (2009).
- [29] A. Monras and F. Illuminati, Phys. Rev. A **83**, 012315 (2011).
- [30] G. Spedalieri, S. L. Braunstein, and S. Pirandola, *Thermal Quantum Metrology*, arXiv: 1602.05958 (2016).
- [31] To derive this transformation rule, consider a single photon emitted in one of the source mode, say c_1 . The optical system transmits this photon with probability η , and transfers it to an environmental mode v_1 with probability $1 - \eta$, i.e.,
- $$|\psi\rangle = c_1^\dagger |0\rangle \rightarrow \left(\sqrt{\eta} a_1^\dagger + \sqrt{1 - \eta} v_1^\dagger \right) |0\rangle.$$
- [32] J. H. Shapiro, IEEE J. Sel. Top. Quantum Electron. **15**, 1547 (2009).
- [33] C. Lupo, V. Giovannetti, S. Pirandola, S. Mancini, and S. Lloyd, Phys. Rev. A **85**, 062314 (2012).
- [34] The imaging system is characterized by the Fresnel number $\mathcal{F} = \ell/x_R$, where ℓ is the size of the source and x_R is the Rayleigh length. For $\mathcal{F} \ll 1$, the imaging system operates in the far-field regime, in which light is attenuated by a factor $\eta \simeq \mathcal{F}$ [32, 33]. By definition, a point-like source is such that its size is much smaller than the typical size of the imaging system, which in our case is the Rayleigh length. It follows that the optical system operates in the far-field regime and the light emitted by the point source is attenuated by a factor $\eta \simeq \mathcal{F} \ll 1$.
- [35] A. Ferraro, S. Olivares, and M. G. A. Paris, *Gaussian States in Quantum Information* (Bibliopolis, Naples, 2005).
- [36] C. Weedbrook, S. Pirandola, R. Garcia-Patron, N. J. Cerf, T. C. Ralph, J. H. Shapiro, and S. Lloyd, Rev. Mod. Phys. **84**, 621 (2012).
- [37] S. Pirandola, G. Spedalieri, S. L. Braunstein, N. J. Cerf, and S. Lloyd, Phys. Rev. Lett. **113**, 140405 (2014).
- [38] G. Adesso and A. Datta, Phys. Rev. Lett. **105**, 030501 (2010).
- [39] P. Giorda, and M. G. A. Paris, Phys. Rev. Lett. **105**, 020503 (2010).
- [40] H. Cramér, *Mathematical Methods of Statistics* (Princeton University, Princeton NJ, 1946).
- [41] J. Rehacek, M. Paur, B. Stoklasa, L. Motka, Z. Hradil, L. L. Sanchez-Soto, *Dispelling Rayleigh's Curse*, arXiv: 1607.05837 (2016).
- [42] R. Nair, M. Tsang, *Ultimate quantum limit on resolution of two thermal point sources*, arXiv: 1604.00937 (2016).